EXHIBIT O

GYNECOLOGY

Characterization of the host inflammatory response following implantation of prolapse mesh in rhesus macaque

Bryan N. Brown, PhD; Deepa Mani, MBBS; Alexis L. Nolfi, BS; Rui Liang, MD; Steven D. Abramowitch, PhD; Pamela A. Moalli, MD, PhD

OBJECTIVE: We sought to determine the predominant cell type (macrophage, T lymphocyte, B lymphocyte, mast cell) within the area of implantation of the prototypical polypropylene mesh, Gynemesh PS (Ethicon, Somerville, NJ); and to determine the phenotypic profile (M1 proinflammatory, M2 antiinflammatory) of the macrophage response to 3 different polypropylene meshes: Gynemesh PS (Ethicon), and 2 lower-weight, higher-porosity meshes, UltraPro (Ethicon) and Restorelle (Coloplast, Humblebaek, Denmark).

STUDY DESIGN: Sacrocolpopexy was performed following hysterectomy in rhesus macaques. Sham-operated animals served as controls. At 12 weeks postsurgery, the vagina-mesh complex was excised and the host inflammatory response was evaluated. Hematoxylin and eosin was used to perform routine histomorphologic evaluation. Identification of leukocyte ($CD45^+$) subsets was performed by immunolabeling for CD68 (macrophage), CD3 (T lymphocyte), CD20 (B lymphocyte), and CD117 (mast cell). M1 and M2 macrophage subsets were identified using immunolabeling ($CD86^+$ and $CD206^+$, respectively), and further evaluation was performed using enzyme-linked immunosorbent assay for 2 M1 (tumor necrosis factor-alpha and interleukin [IL]-12) and 2 M2 (IL-4 and IL-10) cytokines.

RESULTS: Histomorphologic evaluation showed a dense cellular response surrounding each mesh fiber. $CD45^+$ leukocytes accounted for 21.4 ± 5.4% of total cells within the perimesh area captured in a ×20 field, with macrophages as the predominant leukocyte subset (10.5 ± 3.9% of total cells) followed by T lymphocytes (7.3 ± 1.7%), B lymphocytes (3.0 ± 1.2%), and mast cells (0.2 ± 0.2%). The response was observed to be more diffuse with increasing distance from the fiber surface. Few leukocytes of any type were observed in sham-operated animals. Immunolabeling revealed polarization of the macrophage response toward the M1 phenotype in all mesh groups. However, the ratio of M2:M1 macrophages was increased in the fiber area in UltraPro ($P = .033$) and Restorelle ($P = .016$) compared to Gynemesh PS. In addition, a shift toward increased expression of the antiinflammatory cytokine IL-10 was observed in Restorelle as compared to Gynemesh PS ($P = .011$).

CONCLUSION: The host response to mesh consists predominantly of activated, proinflammatory M1 macrophages at 12 weeks postsurgery. However, this response is attenuated with implantation of lighter-weight, higher-porosity mesh. While additional work is required to establish causal relationships, these results suggest a link among the host inflammatory response, mesh textile properties, and clinical outcomes in the repair of pelvic organ prolapse.

Key words: cytokines, inflammatory response, macrophage phenotype, polypropylene mesh, rhesus macaque

Cite this article as: Brown BN, Mani D, Nolfi AL, et al. Characterization of the host inflammatory response following implantation of prolapse mesh in rhesus macaque. Am J Obstet Gynecol 2015;213:668.e1-10.

More than 250,000 women per year in the United States will undergo surgery for the treatment of pelvic organ prolapse, with direct costs totaling >$1 billion.[1-3] Native tissue repair has a recurrence rate of 40% at 2 years[4,5]; therefore, mechanical reinforcement of tissues using synthetic mesh has increased over the last decade.[6] While

From the Departments of Bioengineering (Drs Brown, Abramowitch, and Moalli and Ms Nolfi) and Obstetrics, Gynecology, and Reproductive Sciences (Drs Brown, Liang, Abramowitch, and Moalli), and McGowan Institute for Regenerative Medicine (Drs Brown, Mani, and Moalli), University of Pittsburgh; and Magee–Womens Research Institute (Drs Liang and Moalli), Pittsburgh, PA.

Received April 15, 2015; revised June 21, 2015; accepted Aug. 2, 2015.

This work was supported by National Institutes of Health awards R01 HD061811 (P.A.M.) and K12HD043441 (B.N.B.). The content is solely the responsibility of the authors and does not necessarily represent the official views of the National Institutes of Health. The funding source had no involvement in the study design, collection of data, analysis of data, interpretation of data, writing of the report, or the decision to submit for publication.

The authors report no conflict of interest.

Presented at the Joint Scientific Meeting of the American Urogynecologic Society and International Urogynecologic Association, Washington, DC, July 22-26, 2014.

Corresponding author: Pamela A. Moalli, MD, PhD. pmoalli@mail.magee.edu

0002-9378/$36.00 • • http://dx.doi.org/10.1016/j.ajog.2015.08.002

TABLE 1
Mechanical and structural characteristics associated with each mesh[12,26]

	Gynemesh PS (Ethicon)	UltraPro (Ethicon)	Restorelle (Coloplast)
Weight, g/m^2	44	31	19
Pore size, μm	2240	≥4000[a]	2370
Porosity, %	64 ± 2.1	69 ± 1.8	78 ± 3.0
Stiffness, N/mm	28 ± 2.7	22 ± 2.8	11 ± 0.89

[a] UltraPro contained resorbable component (poliglecaprolactone 25) in addition to polypropylene allowing it to have very large pores (4 mm) when this component is resorbed; values reported with resorbable component dissolved.

Brown. Inflammatory response to prolapse mesh. Am J Obstet Gynecol 2015.

mesh implantation has been shown to improve anatomical outcomes in the anterior and apical compartments, complications are observed, particularly with transvaginal placement,[7-11] including mesh exposure through the vaginal wall, shrinkage, erosion, and pain.

Recent work suggests that mesh exposures may be induced by stress shielding. That is, a mismatch in stiffness between the mesh and tissue lead to degeneration of the underlying vagina and a loss of mechanical integrity over time. This maladaptive remodeling response precipitates atrophy of the smooth muscle layer associated with a decrease in contractility as well as a shift in tissue extracellular matrix composition and a loss of biomechanical integrity.[12-14] Differences in mesh properties (weight, pore size, porosity, stiffness) were shown to be related to the degree to which this degenerative process occurs, with higher-weight, lower-porosity, and increased-stiffness mesh being associated with increased vaginal tissue degradation. Mesh with higher weight, lower porosity, and increased stiffness has also been suggested to result in increased rates of complications in clinical practice.[15,16]

Mesh complications may also be attributable to the inflammatory processes associated with the macrophage-predominated foreign body reaction mounted by the host following implantation. Without question, the long-term presence of activated proinflammatory cells can have a negative impact on the ability of a material to function as intended. However, a number of recent studies have demonstrated that the macrophage response is also an essential component of the process leading to tissue incorporation, and functional remodeling of implanted materials, suggesting the potential for phenotypic dichotomy in the host response.[17,18] Indeed, macrophages have been classified as having diverse and plastic phenotypes along a continuum between M1 (classically activated; proinflammatory) and M2 (alternatively activated; regulatory, homeostatic) extremes.[19-21] An increasing number of studies in the field of biomaterials have begun to apply these paradigms and concepts, showing that macrophage polarization is a predictor of integration following implantation in multiple applications.[18,22-25] However, the macrophage response following implantation of surgical mesh with varying characteristics has not been described. Moreover, limited studies to date have addressed the impact of mesh implantation on the vagina—an organ with an immunologically distinct environment from that of other tissues in which the host response to mesh has been examined.

The objectives of the present study were 2-fold: (1) to determine the predominant cell type (macrophage, T lymphocyte, B lymphocyte, mast cell) within the area of implantation of the prototypical polypropylene mesh, Gynemesh PS (Ethicon, Sommerville, NJ); and (2) to determine the phenotypic profile (M1 proinflammatory, M2 antiinflammatory) of the macrophage response to 3 different polypropylene meshes: Gynemesh PS, and 2 lower-weight, higher-porosity meshes, UltraPro (Ethicon) and Restorelle (Coloplast, Humblebaek, Denmark).

Materials and Methods

Meshes

The test articles consisted of 3 polypropylene meshes with varying textile and mechanical characteristics as previously described.[12,26] Briefly, specific weight and pore size were provided by the manufacturer. Porosity was determined using a custom-designed algorithm (Matlab, Version 8.0; Mathworks, Natick, MA) and stiffness was determined by ball burst testing. Table 1 shows the relevant mechanical and structural characteristics associated with each mesh. Of note, UltraPro is manufactured with an absorbable component (poliglecaprolactone 25) in addition to polypropylene allowing it to have very large pores (4 mm) when this component is fully absorbed.

Animals

The samples for the present study were obtained from a larger study.[12,13]

TABLE 2
Demographic data collected (age, weight, gravidity, and parity)

Groups	Age, y[a]	Parity[b]	Weight, kg[a]	POP-Q stage[b]
Sham	12.6 ± 2.8	3 (2, 6)	7.3 ± 1.4[c]	0 (0, 1)
Gynemesh PS	12.9 ± 2.2	4 (3.8, 5)	8.2 ± 1.6	0 (0, 0)
UltraPro	13.0 ± 2.2	3.5 (2, 5.8)	7.8 ± 1.4	0 (0, 0.25)
Restorelle	13.8 ± 1.7	5 (3, 5.5)	10.0 ± 2.8[c]	0.5 (0, 1.3)
P value[d]	.780	.970	.042	.700

[a] Mean ± SD; [b] Median (first quartile, second quartile); [c] Statistical significance between groups ($P < .05$); [d] Comparison of overall *P* value among groups.

Brown. Inflammatory response to prolapse mesh. Am J Obstet Gynecol 2015.

FIGURE 1
Histologic appearance of sham and mesh implanted tissues

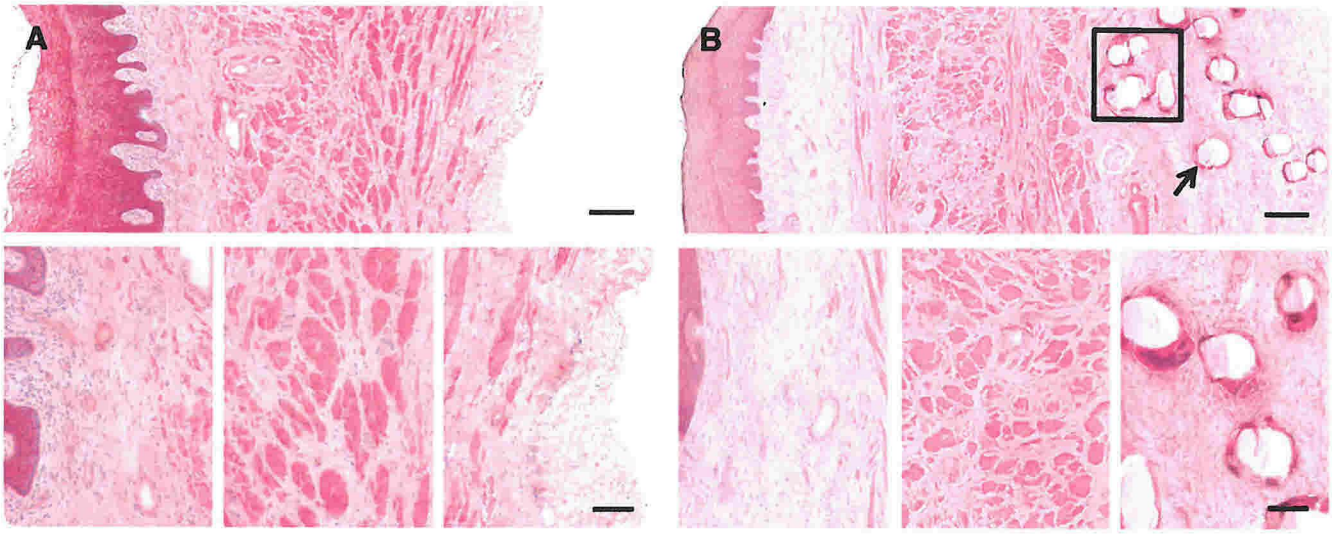

Representative histologic section (hematoxylin and eosin) taken from **A**, sham and **B**, Gynemesh PS groups. Top panels contain full view of histologic section at ×10 original magnification (scale bar = 250 μm). Bottom panels shows higher-magnification images of **A**, subepithelial connective tissues, muscularis layer, and adventitia or **B**, mesh-tissue interface at ×20 original magnification (scale bar = 100 μm). Histomorphologic appearance of response to Gynemesh PS was characteristic of response observed in all mesh-implanted groups. A dense population of mononuclear and multinucleated giant cells can be observed at mesh-tissue interface, decreasing in number with increasing distance from mesh surface. **B**, Box indicates mesh knot and arrow indicates mesh fiber.

Brown. Inflammatory response to prolapse mesh. Am J Obstet Gynecol 2015.

A subset of animals from that study was selected based on the availability of sufficient tissue samples for completion of the assays described in the present study. All animals in this study were maintained and treated according to an approved institutional animal care and use committee protocol and in accordance with the National Institutes of Health Guide for the Care and Use of Laboratory Animals. Demographic data of each animal were collected prior to surgery, including age, weight, gravidity, and parity (Table 2). In all, 32 middle-aged parous rhesus macaques underwent implantation with Gynemesh PS (n = 8), UltraPro (n = 8), Restorelle (n = 8), or sham (n = 8). Mesh was implanted by sacrocolpopexy after an abdominal hysterectomy as previously described.[12,13] Sacrocolpopexy was chosen as observational data suggest that complications related to this procedure are less than those following transvaginal implantation.[11,27]

Sample harvest

At 12 weeks postsurgery, vagina-mesh tissue complexes were harvested as previously described.[12,13] The equivalent tissues were excised in sham-operated animals. A portion of the vagina-mesh complex was embedded in optimal cutting temperature solution (Sakura Finetek USA, Torrence, CA) prior to flash freezing on liquid

FIGURE 2
Immunofluorescent labeling of cells participating in the host response to implanted mesh

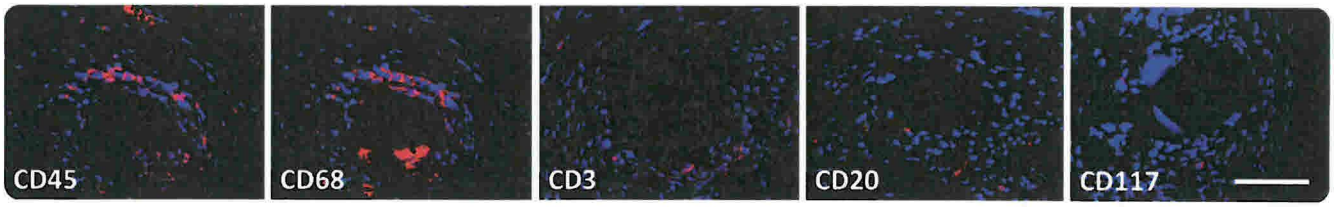

Antibodies for CD45 (panleukocyte), CD68 (macrophage), CD3 (T lymphocyte), CD20 (B lymphocyte), and CD117 (mast cell) markers were used (red). DAPI (blue) was used to label nuclei. Positively labeled cells were predominantly located at mesh surface, with fewer cells with increasing distance. All images at ×40 original magnification, scale bar = 100 μm.

Brown. Inflammatory response to prolapse mesh. Am J Obstet Gynecol 2015.

TABLE 3
Total number of cells and percent surface marker positive cells in ×20 field

Treatment (Gynemesh PS)	Total no. of cells (per ×20 field)	Positive cells (per ×20 field), %
CD45	514 ± 121	21.4 ± 5.4
CD68	510 ± 108	10.5 ± 3.9[a]
CD3	510 ± 114	7.3 ± 1.7[b]
CD20	509 ± 109	3.0 ± 1.2
CD117	508 ± 121	0.2 ± 0.2
P value	1.00[c]	<.001[d]

[a] Significance seen between CD68 and CD20, and CD68 and CD117; [b] Significance seen between CD3 and CD20, and CD3 and CD117; [c] Comparison of *P* value among groups, significant difference if $P < .05$; [d] Comparison among CD68, CD3, CD20, and CD117.

Brown. Inflammatory response to prolapse mesh. Am J Obstet Gynecol 2015.

nitrogen for histologic staining and immunofluorescent labeling. Another portion was harvested and frozen for enzyme-linked immunosorbent assay (ELISA). All samples were stored at −80°C until testing.

Histologic staining and immunofluorescent labeling

Tissue sections (7 μm) were cut and stored at −80°C until use. Slides were thawed at room temperature and stained with hematoxylin and eosin. Slides were dehydrated through a series of graded ethanol (70-100%) and xylenes prior to coverslipping. The histologic appearance of the tissue sections was then evaluated and imaged using a microscope (E600; Nikon, Melville, NY).

For immunolabeling, sections were fixed in 50:50 methanol/acetone for 10 minutes. Antigen retrieval was performed in 10 mmol/L citric acid monohydrate buffer (pH 6.0) at 95°C for 20 minutes. After cooling, the sections were incubated in copper sulfate with ammonium acetate for 20 minutes at 37°C to reduce autofluorescence. The sections were blocked with 1% normal donkey serum, 2% bovine serum albumin, 0.1% Triton-X100, and 0.1% Tween 20 at room temperature for 1 hour. Consecutive sections were then labeled with antibodies specific for leukocytes (CD45), macrophages (CD68), T lymphocytes (CD3), B lymphocytes

FIGURE 3
Immunofluorescent labeling of M1/M2 macrophage response

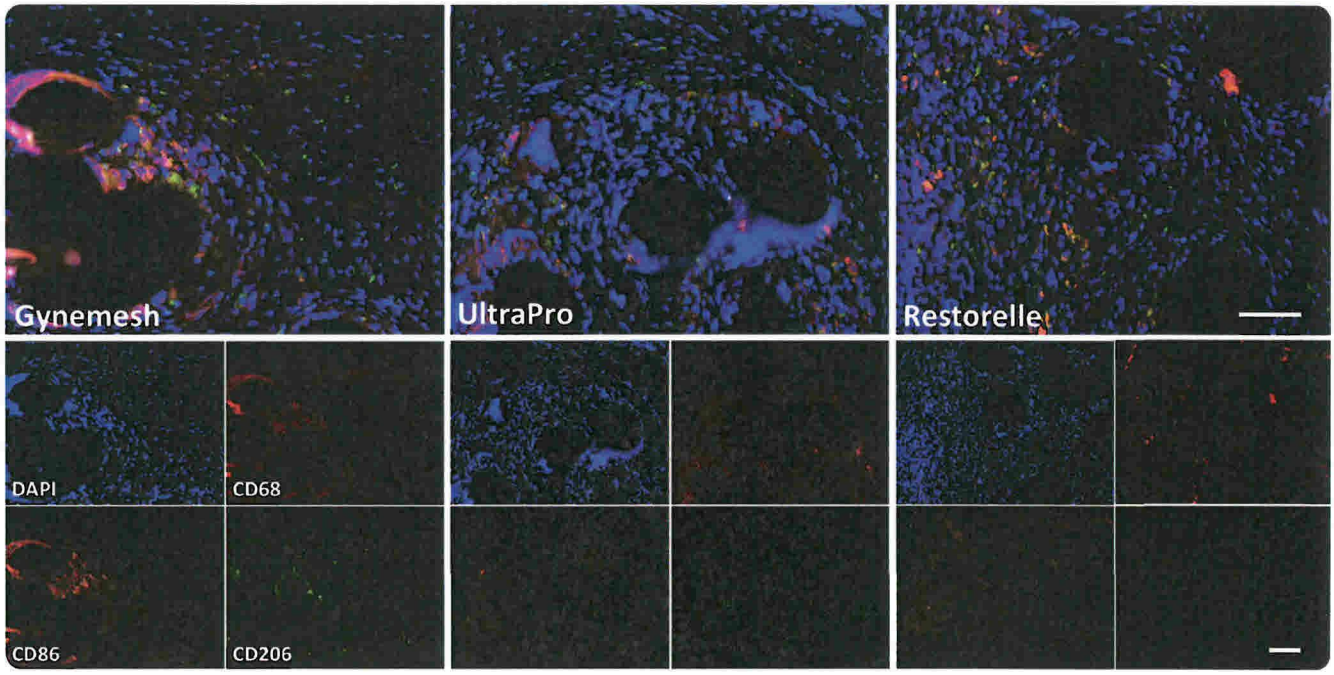

Immunofluorescent labeling with antibodies to CD68 (panmacrophage [red]), CD86 (M1 macrophage [orange]), CD206 (M2 macrophage [green]), and DAPI (nuclei [blue]). Few positive cells were observed in sham-operated animals (not shown). Predominance of M1 macrophage response was observed in Gynemesh PS, UltraPro, and Restorelle groups. Combined fluorescent (top) and individual (bottom) channels. All images at ×20 original magnification (scale bars = 100 μm).

Brown. Inflammatory response to prolapse mesh. Am J Obstet Gynecol 2015.

(CD20), and mast cells (CD117). Primary antibodies, diluted in blocking solution, were applied overnight at 4°C, followed by the corresponding secondary antibodies (product information and dilutions for each primary and secondary antibody are listed in Supplemental Table) and then coverslipped using aqueous mounting media containing 4′,6-diamidino-2-phenylindole; (DAPI; Vectashield with DAPI; Vector Laboratories, Burlingame, CA). Localization of staining to the appropriate regions of lung, liver, kidney, spleen, lymph node, and intestine were used to verify appropriate labeling and incubation of slides without primary antibodies was used as a control. Three representative areas of the mesh-tissue interface were imaged for each individual marker using a ×20 objective on an imaging microscope (Eclipse 90i; Nikon). Quantification of cell types was performed using software (ImageJ; National Institutes of Health, Bethesda, MD). Cell counts were averaged for each sample and expressed as a percentage of total cells within a ×20 field.

Additional sections were triple-labeled with antibodies specific for a panmacrophage marker (CD68), an M1 marker (CD86), and an M2 marker (CD206) as above. Slides were imaged using a ×20 objective at the interface with either single fibers (3 images) or mesh knots (3 images) using a standardized protocol.[28] $CD68^+CD86^+$ cells were considered to have an M1 phenotype and $CD68^+CD206^+$ cells, an M2 phenotype. Cell counts were averaged for each sample and expressed as a percentage of total cells within a ×20 field. Additionally, the ratio of M2:M1 cells was calculated. Because of the scarcity of macrophages in the sham group, the ratio of M2:M1 was not reported. The perimeter of the mesh-tissue interface present in each image was calculated by tracing using ImageJ.

ELISA assay

Frozen tissues were mechanically pulverized and homogenized in a high salt buffer (50 mmol/L Tris base, 150 mmol/L sodium chloride, and 10 μg/mL Halt protease inhibitor cocktail, Pierce Biotechnology, Rockford, IL). After centrifugation, supernatants were collected. Using the DC protein assay (Bio-Rad, Hercules, CA), protein concentrations of all extracts were determined so that all sample volumes contained 40 μg of protein. Amounts of proinflammatory M1 (tumor necrosis factor-alpha, and interleukin [IL]-12p70) and antiinflammatory M2 (IL-10, IL-4) cytokines were assessed using commercially available ELISA assays (Life Technologies, Carlsbad, CA). Both the concentrations of individual cytokines and the ratio of M2/M1 cytokines ([IL-10 + IL-4]/[tumor necrosis factor-alpha + IL-12]) were calculated.

Statistical analysis

Statistical comparisons were made using software (SPSS 18.0; SPSS Inc, Chicago, IL). Primate demographic and immunolabeling data were assessed using 1-way analysis of variance with a Tukey post hoc procedure. As cytokine data were nonparametric, a Kruskal–Wallis test with a Bonferroni-adjusted alpha after pairwise comparisons was performed for each group. A Spearman correlation was used to examine the relationship between the number of M1 and M2 cells and mesh perimeter in each image. A P value $< .05$ was used to determine significance.

RESULTS

Animals had similar age, parity, and pelvic organ prolapse quantification (POP-Q) stage (Table 2). The POP-Q staging methods utilized were the same as that utilized in human beings adjusted to account for the shorter length of the macaque vagina.[29] Animals in the Restorelle group weighed more than the

TABLE 4
Total number of cells, percent of positive cells, and ratio of M2/M1 macrophages seen in ×20 field (fiber)

Treatment	Total no. of cells	M1 positive cells, %	M2 positive cells, %	Ratio, M2/M1
Sham	696 ± 370	0.8 ± 0.7[a]	0.1 ± 0.0[a]	–
Gynemesh PS	642 ± 215	6.8 ± 2.8	3.5 ± 2.2	0.52 ± 0.14[b]
UltraPro	768 ± 232	7.3 ± 2.6	4.6 ± 1.5	0.66 ± 0.08
Restorelle	610 ± 291	7.0 ± 3.7	4.6 ± 2.1	0.67 ± 0.09
P value[c]	.700	<.001	<.001	<.001

[a] Significance seen between sham and Gynemesh PS, sham and UltraPro, and sham and Restorelle; [b] Significance seen between Gynemesh PS and UltraPro, and Gynemesh PS and Restorelle; [c] Comparison of *P* value among groups, significant difference if $P < .05$.

Brown. Inflammatory response to prolapse mesh. Am J Obstet Gynecol 2015.

TABLE 5
Total number of cells, percent of positive cells, and ratio of M2/M1 macrophages seen in ×20 field (knot)

Treatment	Total no. of cells	M1 positive cells, %	M2 positive cells, %	Ratio, M2/M1
Sham	679 ± 327	0.1 ± 0.1[a]	0.1 ± 0.0[a]	–
Gynemesh PS	630 ± 230	8.3 ± 4.7	4.4 ± 2.3	0.57 ± 0.11
UltraPro	722 ± 214	9.2 ± 2.8	5.3 ± 1.0	0.61 ± 0.18
Restorelle	575 ± 104	8.4 ± 2.6	4.9 ± 1.8	0.60 ± 0.11
P value[b]	.620	<.001	<.001	<.001

[a] Significance seen between sham and Gynemesh PS, sham and UltraPro, and sham and Restorelle; [b] Comparison of *P* value among groups, significant difference if $P < .05$.

Brown. Inflammatory response to prolapse mesh. Am J Obstet Gynecol 2015.

TABLE 6
Correlation between percentage of positive cells and mesh area in ×20 image

	M1 cells vs area, %		M2 cells vs area, %	
	Correlation coefficient	*P* value	Correlation coefficient	*P* value
Gynemesh PS	0.39	.006	0.44	.002
UltraPro	0.35	.015	0.23	.113
Restorelle	0.24	.098	0.22	.136
All mesh	0.30	.001	0.23	.006

Brown. Inflammatory response to prolapse mesh. Am J Obstet Gynecol 2015.

other groups ($P = .042$); however, weight did not correlate with any of the measured outcomes ($P > .36$ for all). One animal in the study demonstrated a mesh exposure into the vagina. There were no erosions into adjacent structures.

Histologic analysis

All samples had an intact and qualitatively normal vaginal epithelium as well as a clearly delineated subepithelium, muscular layer, and adventitia (Figure 1). The subepithelial tissues were histologically similar across all groups, with few differences observed between sham and mesh-implanted animals. The largest differences between samples occurred in the smooth muscle layer as previously described, in which the Gynemesh PS induced the most negative impact.[13] All mesh-implanted animals elicited an inflammatory reaction to individual mesh fibers and around knots consisting of a dense infiltrate of mononuclear cells and formation of a fibrous capsule. The response was highly localized with fewer cells observed with increasing distance from the mesh. Multinucleated giant cells were observed at the surface of some, but not all, fibers and knots, regardless of mesh type. The cells at the mesh-tissue interface were predominantly mononuclear in appearance and few, if any, polymorphonuclear cells (neutrophils) were observed. The adventitial layer in sham-operated animals was qualitatively normal, consisting of well-organized loose connective tissue.

Characterization of the immune response to polypropylene mesh

$CD45^+$ cells (panleukocyte) were observed predominantly at the mesh-tissue interface and in the perimesh space in the adventitia with few, if any of these cells within the subepithelium or muscularis of Gynemesh PS–implanted animals indicating a highly localized inflammatory response. $CD68^+$ cells (macrophage) were the immune cell type found in the greatest density immediately surrounding each mesh fiber, while other cells types were fewer in number and found to be located more distantly from the mesh surface (Figure 2). $CD45^+$ cells accounted for 21.4 ± 5.4% of total cells within ×20 fields at the mesh-tissue interface. $CD68^+$ cells (macrophages, 10.5 ± 3.9%) were found to be the predominant leukocyte subtype, followed by $CD3^+$ (T lymphocyte, 7.3 ± 1.7%), $CD20^+$ (B lymphocyte, 3.0 ± 1.2%), and $CD117^+$ (mast, 0.2 ± 0.2%) cells. Although the percentage of macrophages was 44% greater than that of T cells, no significant statistical differences were observed between these two. Both the percentage of macrophages and T lymphocytes were significantly higher than the percentage of B lymphocytes or mast cells (all $P < .001$) (Table 3). No differences in the total number of $DAPI^+$ cells were observed between image sets for each antibody. Few positively labeled cells of any type were observed within the sham (<5 per ×20 field) and, therefore, quantitative analysis of immunolabeled slides was not performed for this group.

Analysis of macrophage phenotype

In all implanted animals, the macrophage response to mesh was observed to be predominantly of the M1 phenotype with fewer cells of either phenotype observed with increasing distance from the mesh surface (Figure 3). In areas with individual fibers, the percentage of M1 cells per ×20 field was increased in mesh-implanted groups (Gynemesh PS

TABLE 7
Individual and ratio values of antiinflammatory and proinflammatory cytokines

Groups	IL-10[a]	IL-4[a]	TNF-alfa[a]	IL-12p70[a]	(IL-10 + IL-4)/(TNF-alfa + IL-12p70)[b]
Sham	1.30 ± 0.31	0.33 ± 0.01	0.38 ± 0.11	0.26 ± 0.06	2.58 ± 0.52
Gynemesh PS	1.03 ± 0.20	0.29 ± 0.08	0.33 ± 0.12	0.27 ± 0.05	2.17 ± 0.78[c]
UltraPro	1.12 ± 0.22	0.27 ± 0.11	0.28 ± 0.15	0.23 ± 0.07	3.01 ± 0.90
Restorelle	1.27 ± 0.22	0.263 ± 0.05	0.26 ± 0.05	0.30 ± 0.15	3.36 ± 0.60[c]
P value[d]	.014	.358	.084	.386	.004

IL, interleukin; *TNF*, tumor necrosis factor.

[a] pg/μg Total protein, mean ± SD; [b] Unitless, mean ± SD; [c] Statistical significance between groups ($P < .05$); [d] Comparison of overall *P* value among groups.

Brown. Inflammatory response to prolapse mesh. Am J Obstet Gynecol 2015.

6.7 ± 2.8%, $P = .003$; UltraPro 7.3 ± 2.6%, $P = .002$; Restorelle 7.0 ± 3.7%, $P = .008$) relative to sham (0.8 ± 0.7%). The percentage of M2 cells was also increased in mesh-implanted groups (Gynemesh PS 3.5 ± 2.2%, $P = .046$; UltraPro 4.6 ± 1.5%, $P = .001$; Restorelle 4.6 ± 2.1%, $P = .001$) relative to sham (0.07 ± 0.03%). The percentage of M2 cells around individual fibers was similar in lighter-weight, higher-porosity meshes (UltraPro, $P = .24$; Restorelle, $P = .32$) as compared to Gynemesh PS. However, the M2/M1 ratio around individual fibers was higher for UltraPro ($P = .033$) and Restorelle ($P = .016$) as compared to Gynemesh PS (Table 4). However, the M2/M1 ratio around individual fibers was higher for UltraPro ($P = .033$) and Restorelle ($P = .016$) as compared to Gynemesh PS (Table 4).

M1 macrophages around mesh knots were increased in the presence of mesh (Gynemesh PS 8.3 ± 4.7%, UltraPro 9.2 ± 2.8%, Restorelle 8.4 ± 2.6%) relative to sham (0.09 ± 0.09%) ($P < .001$). M2 macrophages also increased with mesh implantation (Gynemesh PS 4.4 ± 2.3%, UltraPro 5.3 ± 1.0%, Restorelle 4.94 ± 1.8%) as compared to sham (0.09 ± 0.07%) ($P < .001$). However, in contrast to single fibers, no significant differences in the percentage of M1 and M2 cells or the M2/M1 ratio was observed in areas of mesh knots (Table 5).

The total number of cells within a ×20 field was similar in images containing fibers and knots, despite the increased area occupied by knots as compared to fibers. This suggests a more dense inflammatory response around knots as compared to fibers. Though elevated in images with knots, no statistically significant differences in the percentage of M1 and M2 cells was found between images containing fibers and knots for any mesh ($P = .41$, .18, and .51 for Gynemesh PS, UltraPro, and Restorelle, respectively). A Spearman rho test was used to determine whether there was a correlation between mesh perimeter and percentage of M1 and M2 cells in a given image. Results varied by mesh (Table 6), however, examination of correlations across all mesh types demonstrated a significant correlation between mesh perimeter and the percentage of M1 ($r = .30$, $P < .001$) and M2 ($r = 0.23$, $P = .006$) cells within a given image.

No statistically significant differences were observed between groups for individual cytokines (all $P > .05$) except IL-10 (overall $P = .011$), which was 23% higher in Restorelle as compared to Gynemesh PS ($P = .011$). The ratio of M2/M1 cytokines was also increased in Restorelle-implanted vagina as compared to Gynemesh PS ($P = .003$) (Table 7).

Comment

The present study sought to define the host inflammatory response to 3 polypropylene meshes with distinct textile properties following implantation via sacrocolpopexy in the rhesus macaque. The most significant findings were that, while all mesh materials elicited a predominantly M1 macrophage profile, lower-weight, higher-porosity meshes (UltraPro and Restorelle) elicited a shift in the M2/M1 macrophage ratio in the area around individual mesh fibers. The concentration of antiinflammatory cytokine IL-10 was higher in the Restorelle group as compared to Gynemesh PS, with levels approaching that of the sham-operated group, reflecting differences in the overall local microenvironment associated with the implantation of different mesh types.

This shift in the M2/M1 ratio in the area of individual fibers following the implantation of lighter-weight, higher-porosity meshes, but not following the implantation of a heavier-weight, lower-porosity mesh, is in line with previous observations of abdominal hernia meshes suggesting that "mesh burden," defined as the amount of mesh in contact with tissue, may be a critical factor in the immune response to polypropylene mesh.[30-33] These studies show that polypropylene meshes invariably elicit a foreign body reaction, with the amount of chronic inflammation and scarring proportional to pore size, with an increase in the inflammatory response and scarring over time in meshes with decreased pore size.[32] This phenomenon of increased inflammatory scarring with decreased pore size, termed "bridging fibrosis," suggests that increased fiber density (ie, mesh burden) corresponds to increased inflammatory and fibrotic reactions due to overlap of the host response to multiple individual fibers in close proximity. In the present study, mesh perimeter was found to be positively correlated with the percentage of both M1 and M2 cells present within a given image, suggesting a link between mesh burden and the host inflammatory response exists for meshes implanted in the vagina.

The results of the present study also suggest that macrophage phenotype may influence tissue integration and/or degradation following mesh implantation. Indeed, corresponding to previous findings that the lighter, wider-pore, higher-porosity meshes induced fewer negative effects on the vagina than did Gynemesh PS,[12-14] the present study observed a higher ratio of M2 to M1 phenotype (macrophage polarization) and increased antiinflammatory cytokine IL-10 in the lighter but not in the heavier mesh-implanted vagina. Similar findings of improved material integration and remodeling associated with increased M2 macrophage populations have been observed in a number of other studies such as those in cardiac, dermal, and orthopedic applications of implantable materials of both biologic and synthetic origin.[18,22-25] In a recent study,[18] 15 biologically derived surgical meshes were examined for both histologic outcomes and macrophage polarization profile at 14 and 35 days postimplantation in a partial-thickness rodent abdominal wall defect model. The study showed that the number of M2 cells and the M2:M1 ratio at 14 days postimplantation were strongly correlated with semiquantitative scoring of the histomorphologic appearance of the site of implantation at 14 days and were also predictive of the downstream histologic outcome at 35 days postimplantation. Taken together, this suggests that materials that elicit a higher percentage of M2 cells at the tissue interface may be associated with improved tissue integration and fewer complications in the long term.

There were a number of limitations of the present study. First, only 1 time point was examined, representing a cross-sectional snapshot of a highly dynamic inflammatory process. It should also be noted that, due to the presence of an absorbable component (poliglecaprolactone 25), the mesh burden associated with the UltraPro mesh and the local composition of the material is also dynamic. Thus, the host response to UltraPro may have a transient component not present in the other mesh materials. While statistically significant differences were observed between materials at 90 days, the magnitude of these differences was relatively small. Evaluation of macrophage phenotype at earlier times may have yielded larger differences, but is likely not possible in a primate model due to cost and ethical considerations. Second, only 1 marker of M1 and M2 macrophage phenotypes was used in the present study. It is well known that macrophage phenotype occurs along a spectrum between M1 and M2 with multiple intermediate phenotypes.[21] While this represents the first such attempt to measure macrophage polarization in response to material implantation within the vagina, future studies are needed to better define both the phenotype and the function of the cells participating in the host response to implanted mesh to better understand their impact on tissue integration vs degradation and the occurrence of complications in the long term.[34,35] Third, the present study describes a macrophage-centered approach to the evaluation of the host response at the mesh-tissue interface. Future analyses could specifically evaluate the inflammatory reaction as a function of distance from the mesh surface or within pore spaces. This may be particularly important given that additional cell types, including a notable presence of T lymphocytes, was observed with increasing distance from the mesh surface. Lastly, only mesh introduced by sacrocolpopexy was examined in the present study. Future studies should examine whether there are differences in the host response between mesh introduced by sacrocolpopexy vs transvaginally, and attempt to correlate the findings to the differences in rates of complications observed for these 2 procedures.

In conclusion, the host response to polypropylene mesh consists predominantly of macrophages polarized to a proinflammatory M1 phenotype at 12 weeks postsurgery. However, implantation of lighter-weight, higher-porosity mesh generally attenuated the proinflammatory M1 response. These findings correlate with those of a previous study demonstrating that lighter-weight, higher-porosity mesh was also associated with fewer negative effects on vaginal tissue quality. This suggests that the chronic M1 proinflammatory response to mesh may drive tissue degradation eventually leading to mesh exposures over time similar to what is observed clinically; however, additional work is required to establish a causal relationship. An improved scientific understanding of the mechanisms of the host response to synthetic mesh materials placed in the vagina has the potential to significantly affect the design of next-generation mesh materials, inform clinical practices, and improve outcomes in pelvic floor repair. ■

REFERENCES

1. Subak LL, Waetjen LE, van den Eeden S, Thom DH, Vittinghoff E, Brown JS. Cost of pelvic organ prolapse surgery in the United States. Obstet Gynecol 2001;98:646-51.
2. Boyles SH, Weber AM, Meyn L. Procedures for pelvic organ prolapse in the United States, 1979-1997. Am J Obstet Gynecol 2003;188:108-15.
3. Wu JM, Kawasaki A, Hundley AF, Dieter AA, Myers ER, Sung VW. Predicting the number of women who will undergo incontinence and prolapse surgery, 2010 to 2050. Am J Obstet Gynecol 2011;205:230.e1-5.
4. Barber MD, Brubaker L, Burgio KL, et al. Comparison of 2 transvaginal surgical approaches and perioperative behavioral therapy for apical vaginal prolapse: the OPTIMAL randomized trial. JAMA 2014;311:1023-34.
5. Olsen AL, Smith VJ, Bergstrom JO, Colling JC, Clark AL. Epidemiology of surgically managed pelvic organ prolapse and urinary incontinence. Obstet Gynecol 1997;89:501-6.
6. Jonsson Funk M, Edenfield AL, Pate V, Visco AG, Weidner AC, Wu JM. Trends in use of surgical mesh for pelvic organ prolapse. Am J Obstet Gynecol 2013;208:79.e1-7.
7. Altman D, Vayrynen T, Engh ME, et al. Anterior colporrhaphy versus transvaginal mesh for pelvic-organ prolapse. N Engl J Med 2011;364:1826-36.
8. Diwadkar GB, Barber MD, Feiner B, Maher C, Jelovsek JE. Complication and reoperation rates after apical vaginal prolapse surgical repair: a systematic review. Obstet Gynecol 2009;113:367-73.
9. Feiner B, Jelovsek JE, Maher C. Efficacy and safety of transvaginal mesh kits in the treatment of prolapse of the vaginal apex: a systematic review. BJOG 2009;116:15-24.
10. Maher CM, Feiner B, Baessler K, Glazener CM. Surgical management of pelvic organ prolapse in women: the updated summary version Cochrane review. Int Urogynecol J 2011;22:1445-57.
11. Food and Drug Administration. Urogynecologic Surgical Mesh: Update on the Safety and Effectiveness of Transvaginal Placement for Pelvic Organ Prolapse. FDA Administration E. 2001. Available at: http://www.fda.gov/MedicalDevices/Safety/AlertsandNotices/ucm262435.htm. Accessed April 1, 2015.
12. Feola A, Abramowitch S, Jallah Z, et al. Deterioration in biomechanical properties of the vagina following implantation of a high-stiffness prolapse mesh. BJOG 2013;120:224-32.
13. Liang R, Abramowitch S, Knight K, et al. Vaginal degeneration following implantation of synthetic mesh with increased stiffness. BJOG 2013;120:233-43.
14. Liang R, Zong W, Palcsey S, Abramowitch S, Moalli PA. Impact of prolapse meshes on the metabolism of vaginal extracellular matrix in rhesus macaque. Am J Obstet Gynecol 2015;212:174.e1-7.
15. Mistrangelo E, Mancuso S, Nadalini C, Lijoi D, Costantini S. Rising use of synthetic mesh in transvaginal pelvic reconstructive surgery: a review of the risk of vaginal erosion. J Minim Invasive Gynecol 2007;14:564-9.
16. Kohli N, Walsh PM, Roat TW, Karram MM. Mesh erosion after abdominal sacrocolpopexy. Obstet Gynecol 1998;92:999-1004.
17. Brown BN, Badylak SF. Expanded applications, shifting paradigms and an improved understanding of host-biomaterial interactions. Acta Biomater 2013;9:4948-55.
18. Brown BN, Londono R, Tottey S, et al. Macrophage phenotype as a predictor of constructive remodeling following the implantation of biologically derived surgical mesh materials. Acta Biomater 2012;8:978-87.
19. Mantovani A, Sica A, Sozzani S, Allavena P, Vecchi A, Locati M. The chemokine system in diverse forms of macrophage activation and polarization. Trends Immunol 2004;25:677-86.
20. Mills CD, Kincaid K, Alt JM, Heilman MJ, Hill AM. M-1/M-2 macrophages and the Th1/Th2 paradigm. J Immunol 2000;164:6166-73.
21. Mosser DM, Edwards JP. Exploring the full spectrum of macrophage activation. Nat Rev Immunol 2008;8:958-69.
22. Madden LR, Mortisen DJ, Sussman EM, et al. Proangiogenic scaffolds as functional templates for cardiac tissue engineering. Proc Natl Acad Sci U S A 2010;107:15211-6.

23. Rao AJ, Gibon E, Ma T, Yao Z, Smith RL, Goodman SB. Revision joint replacement, wear particles, and macrophage polarization. Acta Biomater 2012;8:2815-23.
24. Sussman EM, Halpin MC, Muster J, Moon RT, Ratner BD. Porous implants modulate healing and induce shifts in local macrophage polarization in the foreign body reaction. Ann Biomed Eng 2014;42:1508-16.
25. Brown BN, Ratner BD, Goodman SB, Amar S, Badylak SF. Macrophage polarization: an opportunity for improved outcomes in biomaterials and regenerative medicine. Biomaterials 2012;33:3792-802.
26. Feola A, Barone W, Moalli P, Abramowitch S. Characterizing the ex vivo textile and structural properties of synthetic prolapse mesh products. Int Urogynecol J 2013;24:559-64.
27. Maher C, Feiner B, Baessler K, Schmid C. Surgical management of pelvic organ prolapse in women. Cochrane Database Syst Rev 2013;4:CD004014.
28. Wolf MT, Dearth CL, Ranallo CA, et al. Macrophage polarization in response to ECM coated polypropylene mesh. Biomaterials 2014;35:6838-49.
29. Feola A, Abramowitch S, Jones K, Stein S, Moalli P. Parity impacts vaginal mechanical properties and collagen structure in rhesus macaques. Am J Obstet Gynecol 2010;203:595.e1-8.
30. Conze J, Rosch R, Klinge U, et al. Polypropylene in the intra-abdominal position: influence of pore size and surface area. Hernia 2004;8:365-72.
31. Klinge U, Junge K, Stumpf M, Ap AP, Klosterhalfen B. Functional and morphological evaluation of a low-weight, monofilament polypropylene mesh for hernia repair. J Biomed Mater Res 2002;63:129-36.
32. Klinge U, Klosterhalfen B, Birkenhauer V, Junge K, Conze J, Schumpelick V. Impact of polymer pore size on the interface scar formation in a rat model. J Surg Res 2002;103:208-14.
33. Klinge U, Park JK, Klosterhalfen B. The ideal mesh? Pathobiology 2013;80:169-75.
34. Brown BN, Sicari BM, Badylak SF. Rethinking regenerative medicine: a macrophage-centered approach. Front Immunol 2014;5:510.
35. Murray PJ, Allen JE, Biswas SK, et al. Macrophage activation and polarization: nomenclature and experimental guidelines. Immunity 2014;41:14-20.

APPENDIX

SUPPLEMENTAL TABLE

Antibodies used in immunofluorescence labeling

Primary antibody

Name	Dilution	Catalog no.	Clonality	Company
Rabbit anti-CD45	1:600	ab10558	Polyclonal	Abcam
Mouse anti-CD68	1:100	ab955	Monoclonal	Abcam
Rabbit anti-CD3	1:50	A0452	Polyclonal	DAKO
Rabbit anti-CD20	1:50	ab27093	Polyclonal	Abcam
Rabbit anti-CD117	1:50	ab32363	Monoclonal	Abcam
Rabbit anti-CD86	1:150	ab53004	Monoclonal	Abcam
Goat anti-CD206	1:150	sc-34577	Polyclonal	Santa Cruz

Secondary antibody

Name	Dilution	Catalog no.	Wavelength (nm)	Company
Alexa 594 donkey antimouse	1:100	A21203	590/617	Invitrogen
Alexa 568 donkey antirabbit	1:50 (CD3, CD20, and CD117) 1:200 (CD45)	A10042	578/603	Invitrogen
Alexa 488 donkey antigoat	1:250 (CD206)	A11055	488/519	Invitrogen
Alexa 647 donkey antirabbit	1:250 (CD86)	A31573	650/668	Invitrogen

Brown. Inflammatory response to prolapse mesh. Am J Obstet Gynecol 2015.